Mechanics and Mechanical Engineering
Vol. 22, No. 1 (2018) 221–237

https://doi.org/10.2478/mme-2018-0020

An Axisymmetric Contact Problem of an Elastic Layer on a Rigid Circular Base

B. Kebli
S. Berkane
F. Guerrache
Department of Mechanical Engineering
Ecole Nationale Polytechnique, Algiers, Algeria
belkacem.kebli@g.enp.edu.dz
sberkane@uwo.ca
fadila.guerrache@g.enp.edu.dz

Received (18 September 2017)
Revised (14 October 2017)
Accepted (18 November 2017)

An analytical solution is presented to a doubly mixed boundary value problem of an elastic layer partially resting on a rigid smooth base. A circular rigid punch is applied to the upper surface of the medium where the contact is supposed to be smooth. The case of the layer with a cylindrical hole was considered by Toshiaki and all [5]. The studied problem is reduced to a system of dual integral equations using the Boussinesq stress functions and the Hankel integral transforms. With the help of the Gegenbauer formula we get an infinite algebraic system of simultaneous equations for calculating the unknown function of the problem. The truncation method is used for getting the system coefficients. A closed form solution is given for the displacements, stresses and the stress singularity factors. The stresses and displacements are then obtained as Bessel function series. For the numerical application we give some conclusions on the effects of the radius of the punch with the rigid base and the layer thickness on the displacements, stresses, the load and the stress singularity factors are discussed.

Keywords: axisymmetric elastic deformation, contact problem, doubly mixed boundary value, Hankel integral transforms, dual integral equations, infinite algebraic system.

1. Introduction

The contact mechanics is one bases of mechanical engineering and is essential for the security and the reliability of projects design. It treats the calculations implying elastic, viscoelastic or plastic mediums during static or dynamic contacts.

Lebedev and Ufliand [1] studied the problem of pressing a punch of circular cross-section into an elastic layer. They expressed the required displacements and stresses in terms of Neuber-Papkovich auxiliary functions. Which are determined from of Fredholm integral equation with a continuous symmetrical kernel.

The axisymmetric deformation of an elastic layer with a circular line of separation of the boundary conditions on both faces was solved by Zakorko [2]. The corresponding systems of dual integral equations were reduced to a Fredholm integral equations system of the second kind. In the work [3] an axisymmetric contact problem for an elastic layer on a rigid foundation with a cylindrical hole has been considered by Dhaliwal. The problem is reduced to the solution of two simultaneous Fredholm integral equations.

A circular load applied on an elastic layer is developed by Wood [4]. An exact solution was obtained by the Hankel transform method where the stresses and displacements were given in closed form. Toshiaki et al [5] presented the solution of an elastic layer resting on a rigid base with a cylindrical hole whose radius is different from that of the rigid punch applied on the upper surface of the medium. The problem is reduced to the solution of an infinite system of simultaneous equations by assuming that both the contact stress under the punch and the normal displacement in the region of the hole may be expressed as appropriate Bessel series.

Sakamoto [6] considered the axisymmetric problem on an elastic layer weakened by a circular crack subjected to an internal uniform pressure. The study considers the two cases when the surfaces of the layer are free of charge and smoothly clamped. These problems are reduced to dual integral equations which are solved using an infinite system of algebraic equations by the Gegenbauer formula. The work of Sakamoto and Koboyashi [7] an axisymmetric contact problem of an elastic layer subjected to a tensile stress applied to a circular region is presented. Their second paper [8] deals with the contact problem of rigid punch applied on an infinite elastic layer resting on a rigid base with a circular hole. These mixed boundary problems are effectively reduced to an exact solution of infinite systems of simultaneous equation.

In the present work, an analytical solution of an axisymmetric contact problem of an elastic layer on a rigid circular base has been developed. We determine the solution of the elastic problem by the help Hankel integral transform method using the auxiliary Boussinesq stress functions. The doubly mixed boundary value problem is reduced to a system of dual integral equations. The solution procedure is analogous to the elastostatic case treated by Toshiaki [5] and Sakamoto [6]-[8]. The obtained solution is calculated from the coefficients of the infinite system of simultaneous algebraic equations by means of the Gegenbauer expansion formula of the Bessel function. Numerical results are obtained for examining the effects of the radius of the punch with the rigid base and the layer thickness on the displacements, stresses as well as the load and the stress singularity factors.

2. Formulation of the problem and its solution

We use a cylindrical coordinate system (r, θ, z). The Poisson ratio and the Young's modulus of the elastic medium are noted by ν and G, respectively. A general solution of the axisymmetric equilibrium system without torsion can be represented by Boussinesq's harmonic stress functions φ_0, φ_3, where (u_r, v_θ, w_z) denotes the displacement vector and (σ_r, σ_θ, σ_z, τ_{rz}, $\tau_{\theta z}$, $\tau_{r\theta}$) the stress tensor, as follows:

$$2Gu_r = \frac{\partial \varphi_0}{\partial r} + z\frac{\partial \varphi_3}{\partial r} \qquad v_\theta = 0 \tag{1}$$

$$2Gw_z = \frac{\partial \varphi_0}{\partial z} + z\frac{\partial \varphi_3}{\partial z} - (3-4v)\,\varphi_3 \tag{2}$$

$$\sigma_r = \frac{\partial^2 \varphi_0}{\partial r^2} + z\frac{\partial^2 \varphi_3}{\partial r^2} - 2\nu\frac{\partial \varphi_3}{\partial z} \tag{3}$$

$$\sigma_\theta = \frac{\partial \varphi_0}{r\partial r} + z\frac{\partial \varphi_3}{r\partial r} - 2\nu\frac{\partial \varphi_3}{\partial z} \tag{4}$$

$$\sigma_z = \frac{\partial^2 \varphi_0}{\partial z^2} + z\frac{\partial^2 \varphi_3}{\partial z^2} - 2\,(1-\nu)\,\frac{\partial \varphi_3}{\partial z} \tag{5}$$

$$\tau_{rz} = \frac{\partial^2 \varphi_0}{\partial r\partial z} + z\frac{\partial^2 \varphi_3}{\partial r\partial z} - (1-\nu)\,\frac{\partial \varphi_3}{\partial r} \qquad \tau_{r\theta} = \tau_{\theta z} = 0 \tag{6}$$

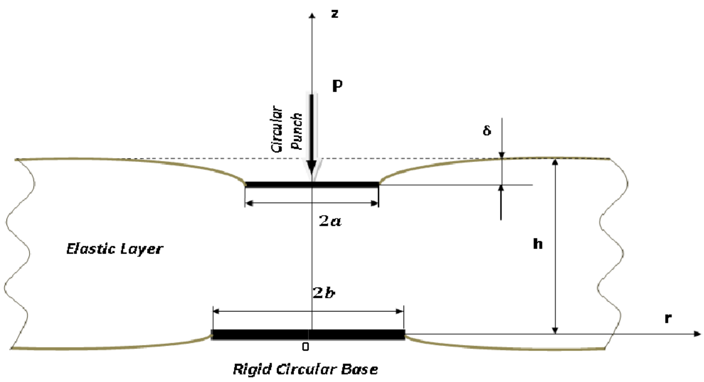

Figure 1 Geometry of the problem

We consider an isotropic elastic layer with thickness h, as shown in Fig. 1 which is indented by a circular area of radius a by the punch with a plane base meanwhile. The layer is resting on a rigid smooth circular base of radius b. If the magnitude of the penetration δ is small by application of an axial force P. The doubly mixed boundary value of the elastic layer can be described by the following equations on the rigid base:

$$(\sigma_z)_{z=0} = 0 \qquad r > b \tag{7}$$

$$(w_z)_{z=0} = 0 \qquad 0 \le r \le b \tag{8}$$

on the upper surface:

$$(\sigma_z)_{z=h} = 0 \qquad r > a \tag{9}$$

$$(w_z)_{z=h} = -\delta \qquad 0 \le r \le a \tag{10}$$

and

$$(\tau_{rz})_{z=0} = (\tau_{rz})_{z=h} = 0 \qquad r \ge 0 \tag{11}$$

All stress components vanish at infinity.

To satisfy the boundary condition (7) we can put the stress function φ_0 and φ_3 in the following forms:

$$\varphi_0 = \int_0^\infty [A(\lambda)\sinh\lambda z + B(\lambda)\cosh\lambda z]\, J_0(\lambda r)\, d\lambda \tag{12}$$

$$\varphi_3 = \int_0^\infty [C(\lambda)\sinh\lambda z + D(\lambda)\cosh\lambda z]\, J_0(\lambda r)\, d\lambda \tag{13}$$

where J_n is a Bessel function of the first kind in order n and $A(\lambda)$, $B(\lambda)$, $C(\lambda)$ and $D(\lambda)$ are unknown functions of λ. Using equations (1) - (6) and (12), (13) the boundary condition (11) allows us to derive the expression:

$$\lambda A(\lambda) = (1-2\nu)\, D(\lambda) \tag{14}$$

$$B(\lambda) = (1-2\nu-\lambda h\coth\lambda h)\, C(\lambda) - \lambda h D(\lambda) \tag{15}$$

From equations (1) - (6) and (12), (15) we obtain the components of displacement and stress:

$$\begin{aligned} 2Gw_z = -\int_0^\infty &\{[(2-2\nu+\lambda h\coth\lambda h)\sinh\lambda z - \lambda z\cosh\lambda z]\, C(\lambda) \\ &+ [(2(1-\nu)\cosh\lambda z - (\lambda z-\lambda h)\sinh\lambda z)\, D(\lambda)]\, J_0(\lambda r)\, d\lambda \end{aligned} \tag{16}$$

$$\begin{aligned} \sigma_r + \sigma_\theta = -\int_0^\infty &\{[(1+2\nu-\lambda h\coth\lambda h)\cosh\lambda z + \lambda z\sinh\lambda z]\, C(\lambda) \\ &+ [((1+2\nu)\sinh\lambda z + (\lambda z-\lambda h)\cosh\lambda z)\, D(\lambda)]\, \lambda J_0(\lambda r)\, d\lambda \end{aligned} \tag{17}$$

$$\begin{aligned} \sigma_r - \sigma_\theta = -\int_0^\infty &\{[(1-2\nu-\lambda h\coth\lambda h)\cosh\lambda z + \lambda z\sinh\lambda z]\, C(\lambda) \\ &+ [((1-2\nu)\sinh\lambda z + (\lambda z-\lambda h)\cosh\lambda z)\, D(\lambda)]\, \lambda J_2(\lambda r)\, d\lambda \end{aligned} \tag{18}$$

$$\begin{aligned} \sigma_z = -\int_0^\infty &\{[(1+\lambda h\coth\lambda h)\cosh\lambda z - \lambda z\sinh\lambda z]\, C(\lambda) \\ &+ [\sinh\lambda z + (\lambda z-\lambda h)\cosh\lambda z]\, D(\lambda)\}\, \lambda J_0(\lambda r)\, d\lambda \end{aligned} \tag{19}$$

$$\begin{aligned} \tau_{rz} = -\int_0^\infty &\{[\lambda z\cosh\lambda z - \lambda z\coth\lambda h\sinh\lambda z]\, C(\lambda) \\ &+ (\lambda z-\lambda h)\sinh\lambda z D(\lambda)]\}\, \lambda J_1(\lambda r)\, d\lambda \end{aligned} \tag{20}$$

Using equations (16) - (20) the boundary conditions (10) to (7) lead to the following system of dual integral equations:

$$(\sigma_z)_{z=0} = -\int_0^\infty [1+\lambda h\coth\lambda h C(\lambda) + \lambda h D(\lambda)]\, \lambda J_0(\lambda r)\, d\lambda = 0 \qquad r > b \tag{21}$$

$$(w_z)_{z=0} = \frac{1-\nu}{G}\int_0^\infty D(\lambda)\, J_0(\lambda r)\, d\lambda = 0 \qquad r \le b \tag{22}$$

$$(\sigma_z)_{z=h} = -\int_0^\infty \left[\left(\cosh\lambda h + \frac{\lambda h}{\sinh\lambda h}\right) C(\lambda)\right.$$
$$\left. + \sinh\lambda h D(\lambda)\right] \lambda J_0(\lambda r)\, d\lambda = 0 \qquad r > a \tag{23}$$

$$(w_z)_{z=h} = -\frac{1-\nu}{G}\int_0^\infty [\sinh\lambda h C(\lambda)$$
$$+ \cosh\lambda h D(\lambda)] J_0(\lambda r)\, d\lambda = -\delta \qquad r \le b \tag{24}$$

A large contribution is made for solving the similar integral equation problems [9]. For the present study we follow the method developed by Sakamoto [6] - [8]. In order to satisfy the two last homogeneous equations of (21) - (24), we can set:

$$\eta\left[\left(\cosh\lambda h + \frac{\lambda h}{\sinh\lambda h}\right) C(\lambda) + \sinh\lambda h D(\lambda)\right] = \sum_{n=0}^{\infty} \alpha_n M_n(\lambda a) \tag{25}$$

$$\eta\left[(1 + \lambda h \coth\lambda h) C(\lambda) + \lambda h D(\lambda)\right] = \sum_{n=0}^{\infty} \beta_n M_n(\lambda b) \tag{26}$$

where:

$$\eta = \frac{1-\nu}{\delta G} \tag{27}$$

$$M_n(\lambda x) = J_{n+\frac{1}{2}}(\lambda x/2)\, J_{-\left(n+\frac{1}{2}\right)}(\lambda x/2) \tag{28}$$

Solving this system of two equations yields the determination of $C(\lambda)$ and $D(\lambda)$:

$$\eta C(\lambda) = \Delta^{-1}(\lambda h) \sum_{n=0}^{\infty} \left[2\lambda h e^{\lambda h}\left(e^{2\lambda h} - 1\right) \alpha_n M_n(\lambda a)\right.$$
$$\left. - \left(e^{2\lambda h} - 1\right)^2 \beta_n M_n(\lambda b)\right] \tag{29}$$

$$\eta D(\lambda) = \Delta^{-1}(\lambda h) \sum_{n=0}^{\infty} \left[-2e^{\lambda h}\left((\lambda h + 1) e^{2\lambda h} + \lambda h - 1\right) \alpha_n M_n(\lambda a)\right.$$
$$\left. + \left(e^{4\lambda h} + 4\lambda h e^{2\lambda h} - 1\right) \beta_n M_n(\lambda b)\right] \tag{30}$$

where:

$$\Delta(\lambda h) = -e^{2\lambda h}\left[e^{2\lambda h} - 2\left(2(\lambda h)^2 + 1\right)\right] - 1 \tag{31}$$

Now if we substitute the expressions of C(λ) and D(λ), given in (16) - (20), into the first two equations of (11), we get:

$$\sum_{n=0}^{\infty} \int_0^\infty \left[\alpha_n f_1(\lambda) M_n(\lambda a) + \beta_n f_2(\lambda) M_n(\lambda b)\right] J_0(\lambda r)\, d\lambda = -1 \quad 0 \le r \le a \tag{32}$$

$$\sum_{n=0}^{\infty} \int_0^\infty \left[\alpha_n f_2(\lambda) M_n(\lambda a) + \beta_n f_2(\lambda) M_n(\lambda b)\right] J_0(\lambda r)\, d\lambda = 0 \quad 0 \le r \le b \tag{33}$$

where:

$$\begin{cases} f_1(\lambda) = \Delta^{-1}(\lambda h)\left(e^{4\lambda h} + 4\lambda h e^{2\lambda h} - 1\right) \\ f_2(\lambda) = \Delta^{-1}(\lambda h)\left[-2e^{\lambda h}\left((1 + \lambda h) e^{2\lambda h} + (\lambda h - 1)\right)\right] \end{cases} \tag{34}$$

Equations (32), (33) are independent of r in their respective intervals. Setting:

$$X_m(\lambda x) = J_m^2\left(\frac{\lambda x}{2}\right) \tag{35}$$

And making use the following Gegenbauer's formula:

$$J_0(\lambda x) = \sum_{m=0}^{\infty}(2-\delta_{0m})\, X_m(\lambda x)\cos m\phi$$

$$r = x\sin(\phi/2) \quad (0 \le r \le x \quad x = a,\, b) \tag{36}$$

where δ_{0m} denotes the Kronecker delta, $\delta_{nm} = \begin{cases} 1, & m = n \\ 0, & m \neq n \end{cases}$
We obtain the following infinite system of simultaneous equations for the determination of α_n and β_n:

$$[\alpha_n f_1(\lambda)\, M_n(\lambda a) + \beta_n f_2(\lambda)\, M_n(\lambda b)]\, X_m(\lambda a)\, d\lambda = -\delta_{0m} \tag{37}$$

$$[\alpha_n f_2(\lambda)\, M_n(\lambda a) + \beta_n f_2(\lambda)\, M_n(\lambda b)]\, X_m(\lambda b)\, d\lambda = 0 \tag{38}$$

2.1. ***Displacements and stresses on two layer boundaries***

The components of displacement on both the upper and lower surfaces of the layer can be expressed as follows:

$$\frac{(w_z)_{z=0}}{\delta} = -H(r-b)\sum_{n=0}^{\infty}\int_0^{\infty}[\alpha_n f_2(\lambda)\, M_n(\lambda a) + \beta_n f_1(\lambda)\, M_n(\lambda b)]\, J_0(\lambda r)\, d\lambda \tag{39}$$

On the upper surface z=h, the components of the displacement can be calculated:

$$\frac{(w_z)_{z=h}}{\delta} = -H(r-a) + H(r-a)\sum_{n=0}^{\infty}\int_0^{\infty}[\alpha_n f_1(\lambda)\, M_n(\lambda a) + \beta_n f_2(\lambda)\, M_n(\lambda b)]\, J_0(\lambda r)\, d\lambda \tag{40}$$

Using the integral formula for the Bessel functions: 6. 522 (11) [10]. Making use of the following integral formula:

$$\int_0^{\infty}\lambda M_n(\lambda x)\, J_0(\lambda r)\, d\lambda = \begin{cases} \frac{2}{\pi r}\frac{T_{2n+1}(r/x)}{\sqrt{x^2-r^2}} & r < x \\ 0 & r > x \end{cases} \tag{41}$$

where T_{2n+1} is the Tchebycheff function of the first kind.
The normal stress on the upper surface z = 0 for r > a can be expressed appropriate Chebyshev series as follows as:

$$\eta(\sigma_z)_{z=0} = -\frac{2}{\pi}H(b-1)\sum_{n=0}^{\infty}\beta_n\frac{T_{2n+1}(r/b)}{r\sqrt{b^2-r^2}} \tag{42}$$

whereas on $z = h$ we obtain:

$$\eta\left(\sigma_z\right)_{z=h} = -\frac{2}{\pi}H\left(a-r\right)\sum_{n=0}^{\infty}\alpha_n\frac{T_{2n+1}\left(r/a\right)}{r\sqrt{a^2-r^2}} \tag{43}$$

The total load P to indent the punch to the magnitude δ is given by

$$P = -2\pi\int_0^a\left(\sigma_z\right)_{z=h}rdr = \frac{4}{\eta}\sum_{n=0}^{\infty}\frac{\left(-1\right)^n}{2n+1}\alpha_n \tag{44}$$

The stress singularity factors corresponding to the studied problem are defined by:

$$S_0 = \lim_{r\to b^-}\sqrt{2\pi\left(r-b\right)}\left(\sigma_z\right)_{z=0} \tag{45}$$

$$S_h = \lim_{r\to a^-}\sqrt{2\pi\left(r-a\right)}\left(\sigma_z\right)_{z=h} \tag{46}$$

Substituting equations (42) and (43) into equations (45), (46). We obtain the simple expression for the stress singularity factors as following:

$$S_0 = \frac{2}{b\sqrt{\pi}}\sum_{n=0}^{\infty}\beta_n \tag{47}$$

$$S_h = \frac{2}{a\sqrt{\pi}}\sum_{n=0}^{\infty}\alpha_n \tag{48}$$

As a particular case, we can find that for b = 0 and$h\to\infty$, equation (19) leads to

$$\sum_{n=0}^{\infty}\alpha_n\int_0^{\infty}M_n\left(\lambda a\right)X_m\left(\lambda a\right)d\lambda = \delta_{0m} \tag{49}$$

From equation (49) we can get $\alpha_0 = a,\;\; \alpha_n = 0,\, (n\geq 1)$

3. Numerical results and discussions

To determine the unknown coefficients α_n and $\beta_n$discussed in previous section, we must evaluate the infinite integrals of the system equations (37) - (38). By separating into the terms obtained by numerical integration and those by an application of the asymptotic expansions of Bessel functions. From the expressions of $f_1\left(\lambda\right)$ and $f_2(\lambda)$ give in (34). It is clear that for large values of λ we get enough $f_1\left(\lambda\right)\to -1$ and $f_2\left(\lambda\right)\to 0$. This allows us to write:

$$\int_0^{\infty}f_1\left(\lambda\right)M_n\left(\lambda x\right)X_m\left(\lambda x\right)d\lambda = \int_0^{\lambda_0}f_1\left(\lambda\right)M_n\left(\lambda x\right)X_m\left(\lambda x\right)d\lambda - \int_{\lambda_0}^{\infty}M_n\left(\lambda x\right)X_m\left(\lambda x\right)d\lambda \tag{50}$$

$$\int_0^\infty f_2(\lambda) M_n(\lambda x) X_m(\lambda x) d\lambda = \int_0^{\lambda_0} f_2(\lambda) M_n(\lambda x) X_m(\lambda x) d\lambda$$

$$x,\, y = a,\, b \tag{51}$$

The first integrals of the night land side of the above expressions are evaluated numerically using the Simpson formula whereas the second one is replaced by the integral of the function equivalent.

Next we evaluate asymptotically the integral term$\int_{\lambda_0}^\infty M_n(\lambda x) X(\lambda x) d\lambda$. As for large value of λ we have:

$$J_\nu(\lambda x) \approx \sqrt{\frac{2}{\pi\lambda x}} \left[\cos\left(\lambda x - \frac{\pi}{2}\nu - \frac{\pi}{4}\right) - \frac{4\nu^2 - 1}{8\lambda x} \sin\left(\lambda x - \frac{\pi}{2}\nu - \frac{\pi}{4}\right)\right.$$

$$\left. +0\left(\frac{1}{(\lambda x)^2}\right)\right] \quad \lambda x \to +\infty \tag{52}$$

$$J_{\left(n+\frac{1}{2}\right)}\left(\frac{\lambda x}{2}\right) J_{-\left(n+\frac{1}{2}\right)}\left(\frac{\lambda x}{2}\right) \approx 4\left(\frac{1}{2}+n\right)^2 \frac{\cos(\lambda x)}{\pi(\lambda x)^2} \tag{53}$$

whereas:

$$M_n(\lambda x) \approx -\frac{8(1+n)}{\pi(\lambda x)^2} \cos(\lambda x) \tag{54}$$

Then $M_n(\lambda x) X_m(\lambda x)$ is replaced by:

$$\frac{4}{\pi^2(\lambda x)^2} \left[\sin(\lambda x) + \frac{(-1)^m}{2}(1 - \cos(2\lambda x))\right] \tag{55}$$

for large values of λ and the integral:

$$\int_{t_0}^\infty \frac{\cos^2(\lambda x_0)}{(\lambda x_0)^2} dt \quad \text{by} \quad \frac{\cos^2 \lambda x_0}{\lambda x_0} + si(2\lambda x_0) \tag{56}$$

Then:

$$\int_{\lambda_0}^\infty M_n(\lambda x) X_n(\lambda x) d\lambda \approx \frac{4}{\pi^2(x)^2} \left\{\frac{\sin(\lambda_0 x)}{\lambda_0} - x ci(\lambda_0 x)\right.$$

$$\left. + \frac{(-1)^m}{2}\left[\frac{1-\cos(2\lambda_0 x)}{\lambda_0} - 2x si(2\lambda_0 x)\right]\right\} \tag{57}$$

where *si(x)* is the integral sine function:

$$si(x) = -\int_x^\infty \frac{\sin\xi}{\xi} d\xi \tag{58}$$

and *ci(x)* is the integral cosine function:

$$ci(x) = -\int_x^\infty \frac{\cos\xi}{\xi} d\xi \tag{59}$$

Table 1 Values of the coefficients α_n and β_n for h/a = 1.5 and various values of b/a

n	b/a = 0.5	b/a = 1	b/a = 1.5
	α_n		
0	0.559686534802502	1.281311717811767	1.644374747440548
1	-0.185395060778207	-0.203638231658882	-0.102050296340474
2	0.029552956378661	0.014286773708200	0.003647691155375
3	-0.003018696960819	0.000239948419853	0.000094166506271
4	0.000208910491890	-0.000105729434747	-0.000001512460679
5	-0.000006932641063	0.000004387723409	-0.000002837293623
6	-0.000002042929074	-0.000003152691474	-0.000004723300180
7	-0.000002352058641	-0.000006872410117	-0.000009595974541
8	-0.000004683009179	-0.000012603386507	-0.000017762314415
9	-0.000003098017624	-0.000008388267814	-0.000011826332774
	β_n		
0	0.619456189051369	1.277824098584786	1.381502620649796
1	-0.011314548473684	-0.207500728123057	-0.813951036152699
2	0.000182590062900	0.014236787062389	0.138492107445660
3	0.000000754790856	0.000252829347999	-0.004749530147052
4	-0.000002379929250	-0.000106730796414	-0.002723247263488
5	-0.000006330790601	0.000004417291304	0.000618631151190
6	-0.000014372442618	-0.000003127411009	-0.000046861951699
7	-0.000029369934242	-0.000006828792265	-0.000007854765221
8	-0.000054618999189	-0.000012521155141	-0.000000079816219
9	-0.000036425537745	-0.000008333309575	-0.000001852011178

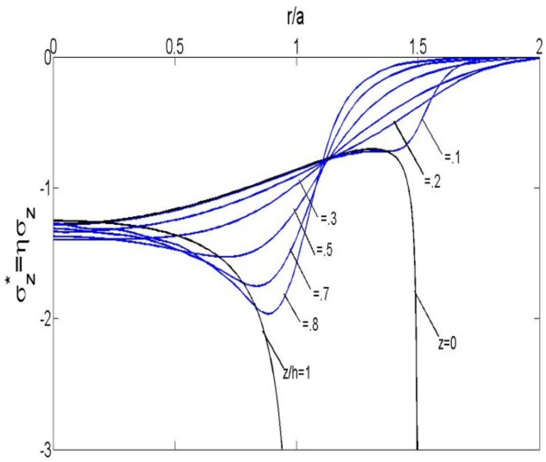

Figure 2 The variation of the distribution of σ_z^* for h/b = 1.5 and b/a = 1.5 with various values of z/a

Table 2 Values of the coefficients α_n and β_n for b/a = 1.5 and various values of h/a

n	h/a = 0.7	h/a = 1	h/a = 1.5
		α_n	
0	2.659907562693490	2.102315861316422	1.644374747440548
1	-0.465369868613824	-0.216242333748549	-0.102050296340474
2	0.038559658922877	0.016086130678807	0.003647691155375
3	0.002026576675632	-0.000132119321970	0.000094166506271
4	-0.000315036921171	-0.000019167988751	-0.000001512460679
5	0.000002557413666	-0.000001442108547	-0.000002837293623
6	-0.000006181312092	-0.000006000199801	-0.000004723300180
7	-0.000014169878542	-0.000011832796019	-0.000009595974541
8	-0.000025796885320	-0.000021886145107	-0.000017762314415
9	-0.000017166183937	-0.000014570262368	-0.000011826332774
		β_n	
0	1.854716535735087	1.575388298969770	1.381502620649796
1	-2.681194107187618	-1.647132725784705	-0.813951036152699
2	0.557344928416927	0.315793975338493	0.138492107445660
3	0.182944146592442	0.035197211736266	-0.004749530147052
4	-0.107398009461012	-0.028323713330607	-0.002723247263488
5	-0.002997896836750	0.003707279724757	0.000618631151190
6	0.0024612211552625	0.001043983655695	-0.000046861951699
7	-0.002089912667773	-0.000466865123625	-0.000007854765221
8	-0.001178413993801	0.000035591438942	-0.000000079816219
9	0.000559177760934	0.000026707047819	-0.000001852011178

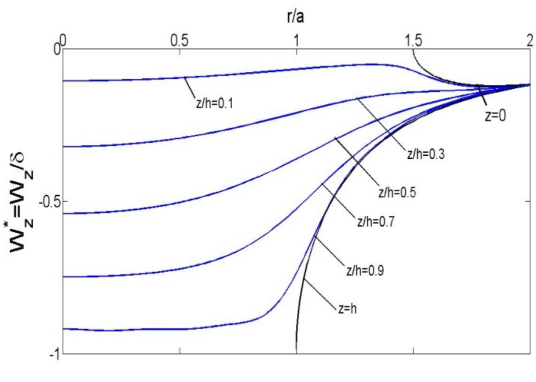

Figure 3 The variation of the distribution of w_z^* for h/b = 1.5 and b/a = 1.5 with various values of z/a

In this study the value $\lambda_0 = 1500$ was used. The coefficients elastics α_n and β_n are shown in the following Tabs. 1–2 of the thickness elastic layer and the radius of the punch with the rigid base.
The distribution of the stresses and the displacements with different values of plan z/a is graphically illustrated in the Figs. 2–3.
Figures 4–5 show the variation of the nondimensional normal stress $(\sigma_z^*)_{z=0}$ for h/a and b/a, respectively. The distribution gets its maximum values at the centre of the rigid base. The stress has an infinite value if r/a = b/a. It decreases with decreasing the layer thickness and the radius of the rigid base.

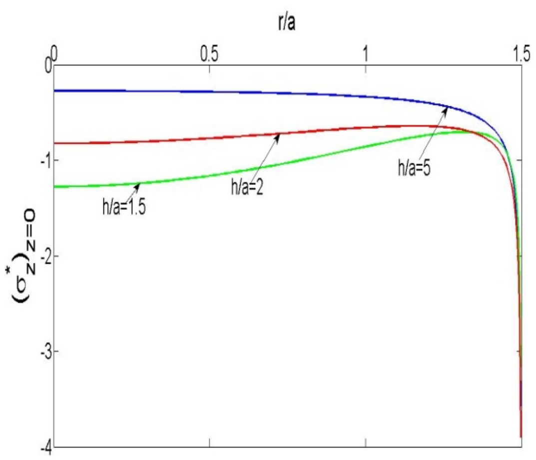

Figure 4 The variation of $(\sigma_z^*)_{z=0}$ for b/a = 1.5 and various values of h/a

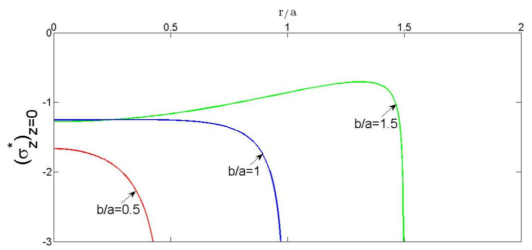

Figure 5 The variation of $(\sigma_z^*)_{z=0}$ for h/a = 1.5 and various values of b/a

The distribution of the nondimensional axial displacement at the edge of the rigid base is given in Fig. 6 with various values of h/a. It is noted that the value are decreasing with increasing the layer thickness and the rigid base radius. Graphically they are illustrated in Fig. 7.

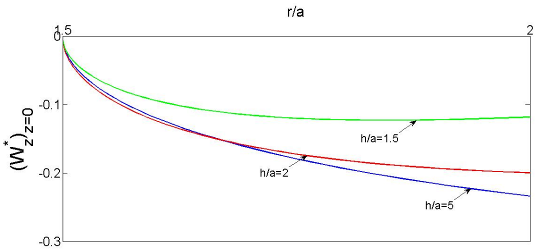

Figure 6 The variation of $(w_z^*)_{z=0}$ for b/a = 1.5 and various values of h/a

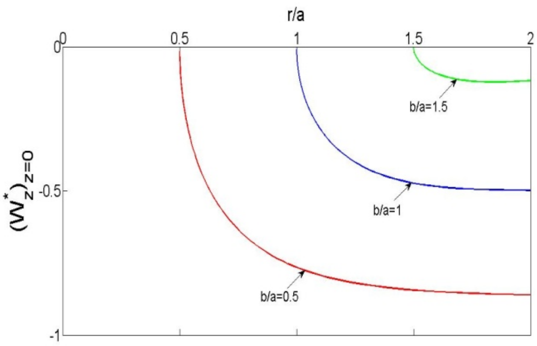

Figure 7 The variation of $(w_z^*)_{z=0}$ for h/a = 1.5 with and various values of b/a

The normal stress at the upper surface can be seen from Figures 8-9. It is shown for various values for h/a and b/a, respectively. The distribution gets its maximum values with the centre of the punch. It decreases with decreasing the thickness of the elastic layer and increasing the radius of the rigid base.

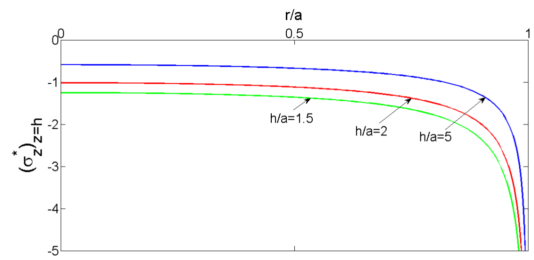

Figure 8 The variation of $(\sigma_z^*)_{z=h}$ for b/a = 1 and various values of h/a

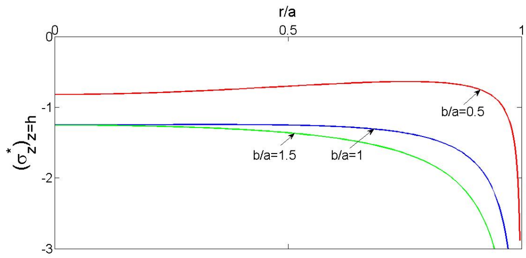

Figure 9 The variation of $(\sigma_z^*)_{z=h}$ for h/a = 1.5 and various values of b/a

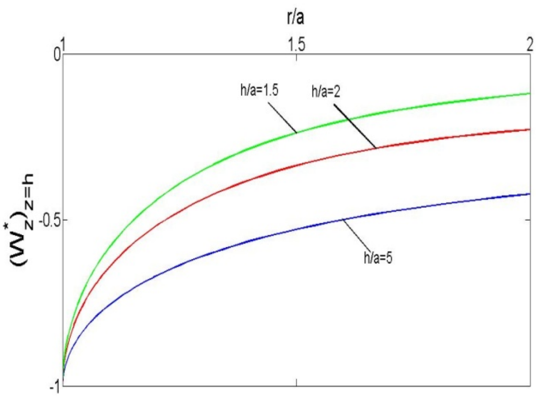

Figure 10 The variation of $(w_z^*)_{z=h}$ for b/a = 1 and various values of h/a

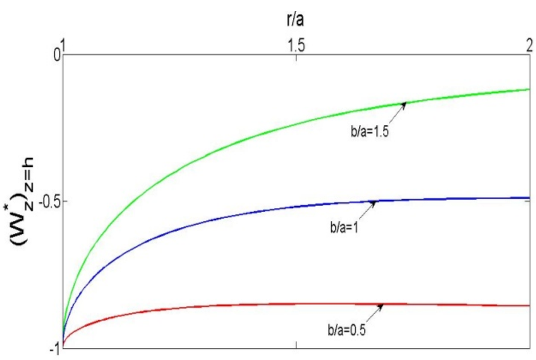

Figure 11 The variation of $(w_z^*)_{z=h}$ for h/a = 1.5 and various values of b/a

The distribution of the displacement for the upper surface is shown from Figures 10-11 with h/a, b/a. It increases with increasing the layer thickness and decreasing the rigid base radius.
The variations of the total load $P^* = \frac{\eta P}{4}$ applied to the punch with the layer thickness and rigid base are mentioned in Figures 12–13. It is noted that the value of P^* increases with decreasing the layer thickness and increasing the rigid base radius.

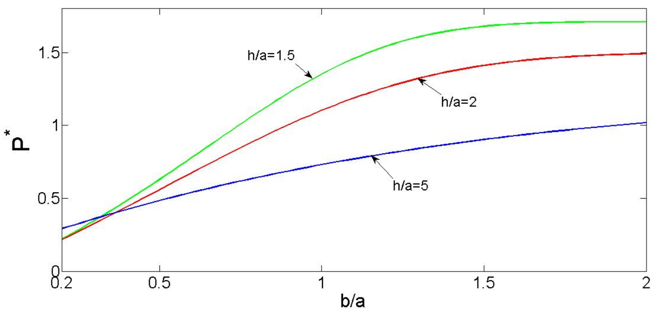

Figure 12 The variation of $P^* = \frac{\eta P}{4}$ for b/a = 0.75 and various values of h/a

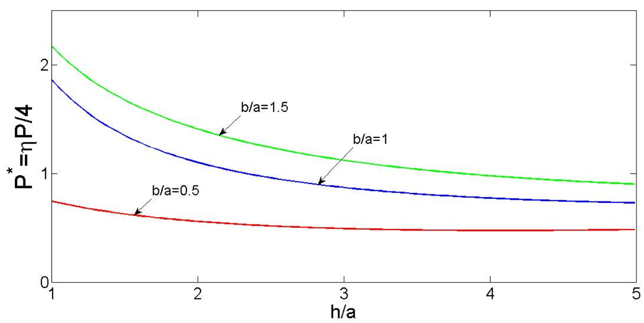

Figure 13 The variation of P^* for h/a = 1.5 and various values of b/a

The variation of the stress singularity factors corresponding to the problem is graphically illustrated in Figures 14-17. The stress singularity factors S_0 and S_h, give a large value with decreasing the layer thickness. It is noted that the value S_0 increases with the rigid base radius, the opposite behaviour is obtained for the case S_h.

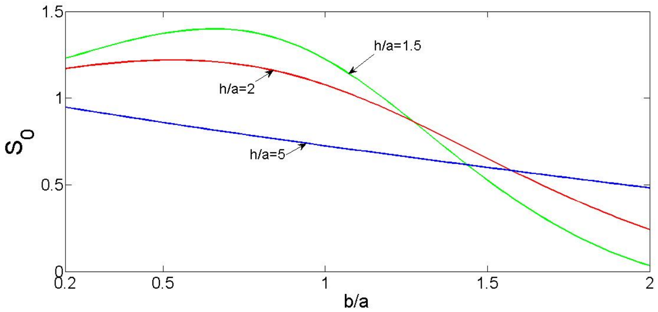

Figure 14 The variation of S_0 for h/a = 1.5 and various values of b/a

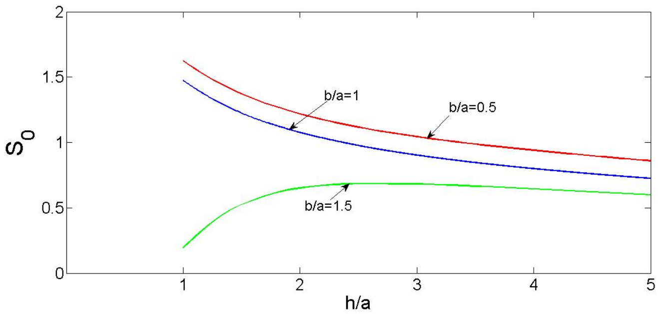

Figure 15 The variation of S_0 for b/a = 0.75 and various values of h/a

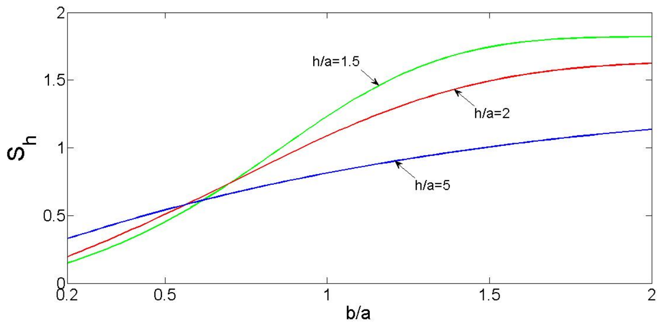

Figure 16 The variation of S_h for b/a = 0.75 and various values of h/a

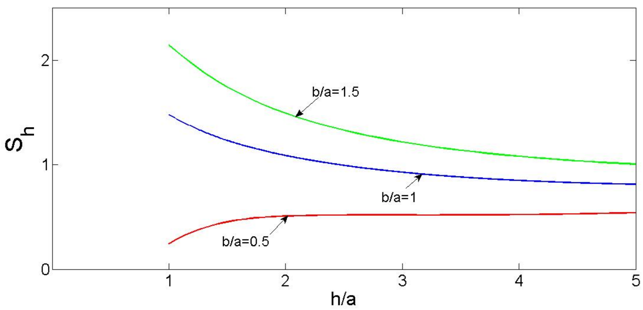

Figure 17 The variation of S_h for h/a = 1.5 and various values of b/a

4. Conclusion

In the present paper, we studied a doubly mixed boundary value problem for an elastic layer. An analytical solution was obtained for the corresponding dual integral equations system through an infinite system of simultaneous equations using the Gegenbauer formula.

The obtained results are summarized as follows:

1. Analytical solution based upon the integral Hankel transforms for contact problem have been developed and utilized.

2. By the truncation method. An infinite algebraic system has been solved with different values of the elastic layer thickness and the rigid base radius.

3. The numerical results revealed the effects of the layer thickness and the radius of the punch with the rigid base on the displacement, the normal stress, as well as on the load and the stress singularity factors.

The graphs obtained are analyzed as follows:

1. The distribution of the stresses and displacements with different values of plan z/b is graphically illustrated.

2. The nondimensional normal stress σ_z^* for h/a and b/a gets its maximum values at the centre of the rigid base. The stress has an infinite value r/a = b/a. It decreases with decreasing layer thickness and the radius of the rigid base.

3. It is noted that, the distribution of the nondimensional displacement at the edge of the rigid base with various values of h/a decreases with decreasing the layer thickness and increasing the rigid base radius.

4. The normal stress at the upper surface for various values for h/a and a/b, respectively. The distribution gets its maximum values with the centre of the punch. It decreases with decreasing of the elastic layer thickness and increasing the rigid base radius.

5. An opposite behaviour is remarked for the distribution of the displacement at the edge of the punch.

6. The variations of the total load P^* applied to the punch with the layer thickness and rigid base as also mentioned. It is noted that the value increases with decreasing the layer thickness and increasing rigid base radius.

7. The variation of the stress singularity factors corresponding to the studied problem is graphically illustrated. The stress singularity factors S_0 and S_h, give a large value with decreasing layer thickness. It is noted that the value S_0 increases with the rigid base radius, the opposite behaviour is obtained for the case S_h.

8. The graphical results illustrated the effects of the layer thickness and the punch radius with the rigid base on the applied load and the stress singularity factors.

References

[1] **Lebedev N.N., Ufliand Ia.S.**: Axisymmetric contact problem for an elastic layer, *PMM*, 22, 3, 320–326, **1958**.

[2] **Zakorko N.V.**: The axisymmetric strain of an elastic layer with a circular line of separation of the boundary conditions on both faces, *PMM,* 38, 1, 131–138, **1974**.

[3] **Dhaliwal, R. S., Singh, B. M.**: Axisymmetric contact problem for an elastic layer on a rigid foundation with a cylindrical hole. *Int.J.Engng Sci.,* 15, 1, 421–428, **1977**.

[4] **Wood, D. M.**: Circular load on elastic layer, *International journal for numerical and analytical methods in geomechanics*, 8, 503–509, **1984**.

[5] **Toshiaki, H., Takao, A., Toshiakaru, S., Takashi, K.:** An axisymmetric contact problem of an elastic layer on a rigid base with a cylindrical hole. *JSME International Journal,* 33, 4, 461–467, **1990**.

[6] **Sakamoto, M.**: An elastic layer with a penny-shaped crack subjected to internal pressure, *JSME Int. J. Ser. A*, 46, 1, 27–36, **2003**.

[7] **Sakamoto, M., Kobayashi, K.**: The axisymmetric contact problem of an elastic layer subjected to a tensile stress applied over a circular region, *Theor. Appl. Mech. Japan.*, 53, 27–36, **2004**.

[8] **Sakamoto, S., Kobayashi, K.**: Axisymmetric indentation of an elastic layer on a rigid foundation with a circular hole, *WIT Trans. Enging. Sci.,* 49, 279–286, **2005**.

[9] **Duffy, D. G.**: Mixed boundary value problems, *Boca Raton*, *Chapman Hall/CRC.*, 457, **2008**.

[10] **Gradshteyn, I. S., Ryzhik, I. M.**: Table of integrals- series and products, *Academic Press, N. Y*, 1221, **2007**.